A real-space rescaling treatment of the spectral properties of a binary crystal in the many-neighbour approximation

1986 J. Phys. C: Solid State Phys. 19 3125

(http://iopscience.iop.org/0022-3719/19/17/009)

J. Phys. C: Solid State Phys. 19 (1986) 3125–3139. Printed in Great Britain

A real-space rescaling treatment of the spectral properties of a binary crystal in the many-neighbour approximation

D A Lavis†‡, S G Davison§ and B W Southern‖

† Department of Applied Mathematics, University of Waterloo, Waterloo, Ontario, Canada N2L 3G1

§ Departments of Applied Mathematics and Physics, University of Waterloo, Waterloo, Ontario, Canada N2L 3G1

‖ Department of Physics, University of Manitoba, Winnipeg, Manitoba, Canada R3T 2N2

Received 30 July 1985

Abstract. An exact real-space rescaling transformation is used to calculate the Green functions and densities of states for a one-dimensional binary system with long-range exponentially decaying interactions between the atoms. The model is applied to both diatomic and s–p hybrid crystals.

1. Introduction

Recent work (Southern *et al* 1983a, b, Langlois *et al* 1983, Tremblay and Southern 1983, Lavis *et al* 1985) has demonstrated the effectiveness of the real-space rescaling approach for the study of tight-binding systems. The procedure can be applied to a wide range of problems and provides a direct method of calculating Green functions (GFs). The basic idea is to take equations which describe a system with N degrees of freedom and to perform a transformation in which the number of degrees of freedom is reduced. A set of relationships, or recurrence equations, is obtained between the renormalised energy parameters and the original set. Iteration of these equations leads to an effective diagonalisation of the GF matrix and the diagonal GFs are obtained from the limiting values of the renormalised parameters. If the diagonal GFs are analytically continued into the complex z plane, where $z = E + i\theta$ and E is the energy, the localised states will appear as isolated singularities on the real axis and extended states will appear as branch cuts on the real axis (Economou 1983).

In this work we shall be primarily concerned with a binary system of alternating A and B atoms on a one-dimensional lattice with long-range exponentially decaying interactions, although the method can be used for more general situations. We first apply a transformation which decomposes the system into two non-interacting homogeneous monatomic systems. At this stage it is possible, in some special cases, to relate the properties of the system to those of a monatomic system using a two-valued mapping. We shall use this to extract analytic formulae for band edges and, in some cases, for

‡ On leave from the Department of Mathematics, King's College London, The Strand, London WC2R 2LS, UK.

0022-3719/86/173125 + 15 $02.50

densities of states (DOS). In general the interactions in the new decoupled systems are of a more complicated form, but we shall show that this form is invariant under the rescaling procedure of Southern *et al* (1983b). This allows us to obtain the spectral properties of the original system. The outline of the paper is as follows. In § 2 we consider a monatomic system in the many-neighbour approximation (MNA) as introduced by Davison and Taylor (1969) and describe the rescaling treatment of this model which is needed for the development of a mapping to the diatomic system later in the paper. In § 3 we describe the general diatomic model, implement the one-step transformation to decoupled systems of A and B atoms, and develop the scaling equations. In § 4 we apply the model to crystals of A and B atoms with s orbitals and alternating s and p orbitals, as developed by Davison (1972). In § 5 an application to the s–p hybrid model of Davison and Foo (1976) is considered and our conclusions are presented in § 6.

2. The general monatomic chain

We consider the generalised monatomic tight-binding system with Hamiltonian

$$H_0 = \sum_{s=-\infty}^{\infty} \left(|s\rangle \varepsilon_0 \langle s| + \sum_{n=1}^{\infty} (|s\rangle U^{(n)} \langle s+n| + |s+n\rangle U^{(n)} \langle s|) \right). \tag{1}$$

The spectral properties of the atom at site s can be obtained from the diagonal element $\langle s|G_0|s\rangle$ of the lattice GF operator $G_0 = (zI - H_0)^{-1}$, where I is the identity operator and $z = E + i\theta$, E being the energy. The matrix elements $G_0(s, m) = \langle s|G_0|m\rangle$ of G_0 are given by

$$(z - \varepsilon_0)G_0(s, m) - \sum_{n=1}^{\infty} U^{(n)}(G_0(s+n, m) + G_0(s-n, m)) = \delta_{s,m}. \tag{2}$$

Since the chain is homogeneous we can, without loss of generality, set $m = 0$ and rewrite equations (2) in the form

$$G_0(s, 0) - \sum_{n=1}^{\infty} x_n(G_0(s+n, 0) + G_0(s-n, 0)) = \alpha_s \tag{3}$$

where

$$x_n = U^{(n)}/(z - \varepsilon_0) \tag{4a}$$

$$\alpha_s = \delta_{s,0}/(z - \varepsilon_0). \tag{4b}$$

We now apply a rescaling transformation to equation (3) which decouples alternate sites of the lattice. The transformation is applied iteratively with the even-numbered sites retained and relabelled at each stage of the procedure in order to map the system into an identical system with half as many sites. This rescaling method is described in detail by Southern *et al* (1983b). They have derived the formulae for the rescaled energy parameters which, in terms of our notation, can be expressed in the form

$$x_n' = \frac{2x_{2n} + \Psi_n(x, x) + 2\Phi_n(x, x)}{1 - 2\Phi_0(x, x)} \qquad n > 0 \tag{5a}$$

$$\alpha_0' = \frac{\alpha_0 + 2\Phi_0(x, \alpha)}{1 - 2\Phi_0(x, x)} \tag{5b}$$

$$\alpha_s' = \frac{\alpha_{2s} - \alpha_0 x_{2s} + \Psi_s(x, \alpha) + \Phi_s(x, \alpha) + \Phi_s(\alpha, x)}{1 - 2\Phi_0(x, x)} \qquad s > 0 \qquad (5c)$$

where $\alpha'_{-s} = \alpha'_s$ and

$$\Psi_s(a, b) = \sum_{j=1}^{2s-1} (-1)^{j+1} a_j b_{2s-j} \qquad s > 0 \qquad (6a)$$

$$\Phi_s(a, b) = \sum_{j=1}^{\infty} (-1)^{j+1} a_j b_{2s+j} \qquad s \geqslant 0. \qquad (6b)$$

Successive application of equations (5) yields a sequence $x_n^{(k)}$, $\alpha_s^{(k)}$, $k = 0, 1, 2, \ldots$ of parameter values beginning at some $x_n^{(0)} = x_n$, $\alpha_s^{(0)} = \alpha_s$, given by equations (4). If

$$\lim_{k \to \infty} x_n^{(k)} = 0 \qquad n = 1, 2, \ldots \qquad (7a)$$

a condition which can be checked during numerical implementation, it follows that

$$G_0(0, 0) = \lim_{k \to \infty} \alpha_0^{(k)}. \qquad (7b)$$

The DOS can be obtained in the usual way from the imaginary part of $G_0(0, 0)$. This scaling procedure is independent of the form of the interaction energies $\{U^{(n)}\}$. It is, however, clear that for any practical application of the procedure we need to reduce the infinite set of parameters to a finite set. This can be accomplished by either (a) taking a model with non-zero interactions extending to only a finite number of neighbouring sites or (b) retaining interactions to any range but introducing some relationship between the interactions. An example of the first of these options is the work of Southern *et al* (1983b), where interactions extending either only as far as nearest neighbours (NN) or next NN are considered.

An MNA for a monatomic chain was introduced by Davison and Taylor (1969). The basis of their model is to take

$$U^{(n)} = U\rho^{n-1} \qquad (8)$$

for some parameters U and ρ, where $|\rho| < 1$. The application of the rescaling method to this model will be seen as an example of option (b), described above. From equation (4*a*)

$$x_n = x\rho^{n-1} \qquad (9)$$

where

$$x = U/(z - \varepsilon_0). \qquad (10)$$

For scaling purposes we also write

$$\alpha_s = \beta\rho^{|s|-1} \qquad s \neq 0 \qquad (11)$$

although the initial value of β is zero. The series in equation (5) are now geometric and we obtain the scaling equations

$$\rho^1 = \rho^2 \qquad (12a)$$

$$x' = [2x\rho(1 + \rho^2) + x^2(1 + 3\rho^2)]/\Lambda \qquad (12b)$$

$$\alpha_0' = [\alpha_0(1 + \rho^2) + 2x\beta]/\Lambda \qquad (12c)$$

$$\beta' = [\rho(\beta - \alpha_0 x)(1 + \rho^2) + x\beta(1 + 3\rho^2)]/\Lambda \tag{12d}$$

where

$$\Lambda = (1 + \rho^2) - 2x^2. \tag{13}$$

In the (x, ρ) plane $\rho = 0$ is an invariant line of the transformation (12). It corresponds to the NN problem solved by Southern *et al* (1983b) in which $\beta' = \beta = 0$. Equations (12*a*, *b*) possess a fixed point $\rho = 0$, $x = \frac{1}{2}$ which is approached along an invariant line $x = (1 - \rho)/2$. This line is reached from initial values which satisfy the equations

$$x = (\pm 1 - \rho)/2. \tag{14}$$

If the initial value of x is such that

$$-(1 + \rho)/2 < x < (1 - \rho)/2 \tag{15}$$

then x iterates monotonically to zero, and α_0' in equation (12*c*) converges to a limiting real value. If, on the other hand, the initial value of x neither satisfies equation (15) nor lies on the lines (14) then x' behaves chaotically under iteration and α_0' does not converge.

The lines given by equations (14) are the band edges derived by Davison and Taylor (1969). They can also be obtained by using the change of variable given by

$$x = -\rho + x_1(1 - \rho^2)/(1 - 2\rho x_1) \tag{16}$$

when equation (12*a*) takes the form

$$x_1' = x_1^2/(1 - 2x_1^2) \tag{17}$$

which is the scaling equation for the NN problem. Since the band edges for this problem lie at $x_1 = \pm\frac{1}{2}$ we can obtain equations (14) by substituting these values in equation (16). The diagonal GF $G_1(0, 0)$ for the MNA has been obtained recently, using Fourier transform methods (Davison *et al* 1986). It takes the form

$$G_1(0, 0) = \frac{\alpha_0}{(x + \rho)} \{\rho + [x^{-1} - 2(1 - \rho)^{-1}]^{-1/2}[x^{-1} + 2(1 + \rho)^{-1}]^{-1/2}\}. \tag{18}$$

Numerical implementation of the scaling equations yields results identical to those obtained from equation (18). The NN case of equation (18) with $\rho = 0$ has been derived analytically from the scaling procedure by Lavis *et al* (1985).

3. The diatomic chain

We consider the diatomic chain shown in figure 1 with Hamiltonian

$$H_2 = \sum_{s=-\infty}^{\infty} [|\mathrm{A}; s\rangle \varepsilon_{\mathrm{A}} \langle \mathrm{A}; s| + |\mathrm{B}; s\rangle \varepsilon_{\mathrm{B}} \langle \mathrm{B}; s|)$$

$$+ \sum_{n=1}^{\infty} (|\mathrm{A}; s\rangle V_{\mathrm{AA}}^{(n)} \langle \mathrm{A}; s + n| + |\mathrm{A}; s + n\rangle V_{\mathrm{AA}}^{(n)} \langle \mathrm{A}; s|)$$

$$+ \sum_{n=1}^{\infty} (|\mathrm{B}; s\rangle V_{\mathrm{BB}}^{(n)} \langle \mathrm{B}; s + n| + |\mathrm{B}; s + n\rangle V_{\mathrm{BB}}^{(n)} \langle \mathrm{B}; s|)$$

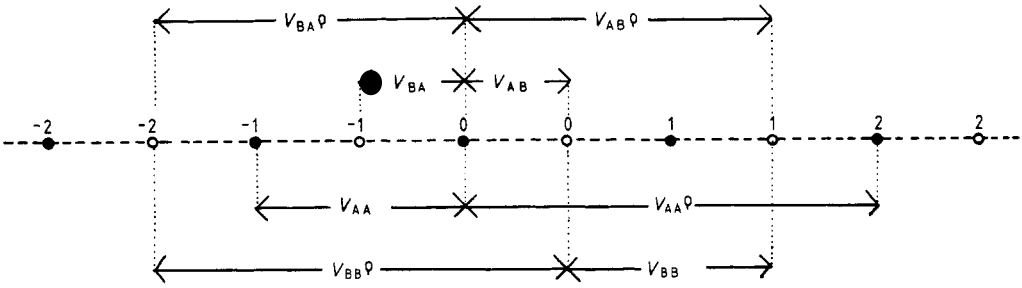

Figure 1. The diatomic lattice. Full circles, A atoms with self-energy ε_A; open circles, B atoms with self-energy ε_B. Interaction energies are indicated and the sites are labelled in pairs. Each pair represents a single atom for the s–p hybrid model.

$$+\sum_{n=0}^{\infty}(|A;s\rangle V_{AB}^{(n)}\langle B;s+n| + |B;s+n\rangle V_{AB}^{(n)}\langle A;s|)$$

$$+\sum_{n=1}^{\infty}(|B;s\rangle V_{BA}^{(n)}\langle A;s+n| + |A;s+n\rangle V_{BA}^{(n)}\langle B;s|)] \tag{19}$$

where

$$\left.\begin{aligned} &V_{AB}^{(n)} = V_{AB}\rho^n \qquad n = 0,1,2,\ldots \\ &V_{BA}^{(n)} = V_{BA}\rho^{n-1} \qquad V_{AA}^{(n)} = V_{AA}\rho^{n-1} \qquad V_{BB}^{(n)} = V_{BB}\rho^{n-1} \qquad n = 1,2,\ldots. \end{aligned}\right\} \tag{20}$$

In this case we have four sets of equations for the elements $G_{CD}(s,m) = \langle C;s|G_2|D;m\rangle$ $(C,D = A,B)$ of the GF operator $G_2 = (zI - H_2)^{-1}$. To these sets of equations we apply an initial transformation equivalent to a block diagonalisation of the matrix into a block associated with the A sites and a block associated with the B sites. The result of this procedure is that we obtain the independent sets of equations

$$G_{CC}(s,0) - \sum_{n=1}^{\infty} x_n(G_{CC}(s+n,0) + G_{CC}(s-n,0)) = \alpha_s^{(C)}$$

$$C = A,B \tag{21}$$

where

$$x_n = x\rho^{n-1} + y(n-1)\rho^{n-2} \tag{22a}$$

$$\alpha_s^{(C)} = \beta_C\rho^{|s|-1} + \gamma_C(|s|-1)\rho^{|s|-2} \qquad s \neq 0, C = A,B \tag{22b}$$

$$x = [V_{AA}(z-\varepsilon_B) + V_{BB}(z-\varepsilon_A) + V_{AB}V_{BA} + \rho W]/Z \tag{23a}$$

$$y = (\rho V_{AB}V_{BA} - V_{AA}V_{BB})/Z \tag{23b}$$

$$\alpha_0^{(A)} = (z-\varepsilon_B)/Z \tag{23c}$$

$$\alpha_0^{(B)} = (z-\varepsilon_A)/Z \tag{23d}$$

$$\beta_A = -V_{BB}/Z \tag{23e}$$

$$\beta_B = -V_{AA}/Z \tag{23f}$$

$$W = (V_{AB}^2 + V_{BA}^2 - 2V_{AA}V_{BB})/(1-\rho^2) \tag{24a}$$

$$Z = (z-\varepsilon_A)(z-\varepsilon_B) - W. \tag{24b}$$

The parameters γ_A and γ_B are zero, but have been included because, under the scaling procedure now to be introduced, they will, in general, become non-zero. At this point we could solve for $G_{CC}(s, 0)$, given by equations (21), using Fourier transform methods. This is possible because of the exponential form of the interactions given by equations (20). However, we shall use the rescaling procedure described in § 2, since it is not restricted to interactions of this form, although it is simpler in this case.

The two sets of equations (21) are each of the form of equations (3) and we apply the rescaling procedure given by equation (5). In this case the interactions are given by equations (22), which are a more general form of MNA than that represented by the corresponding equations (9) and (11). This means that the scaling equations will be more general than those given by equations (12) and take the form

$$\rho' = \rho^2 \tag{25a}$$

$$x' = [2(x\rho + y)(1 + \rho^2)^3 + x^2(1 + 3\rho^2)(1 + \rho^2)^2 + 4xy\rho(1 + \rho^2) - 2y^2\rho^2(3 + \rho^2)]/\Omega \tag{25b}$$

$$y' = y(1 + \rho^2)[(4\rho^2 + 2x\rho - y)(1 + \rho^2)^2 + 4\rho^3 x(1 + \rho^2) - 4y\rho^4]/\Omega \tag{25c}$$

$$\alpha_0^{(C)'} = [\alpha_0^{(C)}(1 + \rho^2)^3 + 2x\beta_C(1 + \rho^2)^2 - 2\rho(y\beta_C + x\gamma_C)(1 + \rho^2) - 2y\gamma_C(1 - \rho^2)]/\Omega \qquad C = A, B \tag{25d}$$

$$\beta_C' = [(\beta_C\rho + \gamma_C - \alpha_0^{(C)}(x\rho + y)(1 + \rho^2)^3 + 2\rho(y\beta_C + x\gamma_C)(1 + \rho^2) + x\beta_C(1 + 3\rho^2)(1 + \rho^2)^2 - 2y\gamma_C\rho^2(3 + \rho^2)]/\Omega \qquad C = A, B \tag{25e}$$

$$\gamma_C' = (1 + \rho^2)[2\rho^2(\gamma_C - y\alpha_0^{(C)})(1 + \rho^2)^2 + [\rho(y\beta_C + x\gamma_C) - y\gamma_C](1 + \rho^2)^2 + 2\rho^3(\gamma_C x + \beta_C y)(1 + \rho^2) - 4\rho^4\gamma_C y\}/\Omega \qquad C = A, B \tag{25f}$$

where

$$\Omega = (1 + \rho^2)^3 - 2x^2(1 + \rho^2)^2 + 4xy\rho(1 + \rho^2) + 2y^2(1 - \rho^2). \tag{26}$$

From equation (25*a*) we see that ρ again iterates to zero and the problem is controlled by the fixed points of the next-NN problem, which are discussed in § 5. We can recover the results for the MNA on a monatomic chain by setting $V_{AB} = V_{BA} = 0$, in which case we have two independent chains. Although this special case provides a useful check on our numerical procedure, the scaling equations (25) do not immediately reduce to equations (12) because of our initial transformation. They do, however, for the chain of A atoms if we also set $V_{BB} = 0$ and similarly for the B atoms if we set $V_{AA} = 0$.

The procedure described in this section can be applied with arbitrary choices for the energy parameters $\varepsilon_A, \varepsilon_B, V_{AA}, V_{BB}, V_{AB}, V_{BA}$. In the following sections we shall consider some particular applications of the model. In some of these, direct analytic information can be derived by obtaining relationships with the monatomic MNA.

4. s-orbital and s–p-orbital models

In order to facilitate the discussion of the initial transformation of our model we chose to label the sites in pairs and to define the MNA based on pairs of sites. In this section a

single-site labelling is preferable. We therefore define a new many-neighbour parameter η by

$$\rho = \eta^2 \tag{27a}$$

with

$$V_{AA} = \eta \bar{V}_{AA} \tag{27b}$$

$$V_{BB} = \eta \bar{V}_{BB}. \tag{27c}$$

In this section we consider two models: case (a) where each atom has only an s orbital; case (b) where each A atom has an s orbital and each B atom has a p orbital. This means that

$$V_{BA} = V \tag{28a}$$

$$V_{AB} = \sigma V \tag{28b}$$

for some parameter V, where

$$\sigma = \begin{cases} +1 & \text{for case (a)} \\ -1 & \text{for case (b).} \end{cases} \tag{29}$$

With this choice of parameters and $\bar{V}_{AA}$ and $\bar{V}_{BB}$ taking the same sign for case (a) and different signs for case (b), the rescaling method of § 3 allows us to compute the partial

$$\bar{V}_{AA} = V \tag{30a}$$

$$\bar{V}_{BB} = \sigma V \tag{30b}$$

have been considered by Davison (1972). In these circumstances it will be seen, from equation (23*b*), that the initial value of y is zero and, since the initial values of γ_A and γ_B are in any case zero, these three parameters will remain zero under iteration. This means that the rescaling equations will be of the form of those for the monatomic chain, given by equations (12), with $\rho = \eta^2$ and $\beta = \beta_A$ and β_B, $\alpha_0 = \alpha_0^{(A)}$ and $\alpha_0^{(B)}$. The difference between this situation and that of the monatomic chain is in the initial conditions. From equations (23) and (27)–(30) these can be expressed in the form

$$x = [\zeta\eta(1+\sigma)(1+\eta^2) + \varphi\eta(1-\sigma)(1-\eta^2) + \sigma + 3\eta^2]/\chi_\sigma \tag{31a}$$

$$\alpha_0^{(A)} = (\zeta + \varphi)(1 + \sigma\eta^2)/V\chi_\sigma \tag{31b}$$

$$\alpha_0^{(B)} = (\zeta - \varphi)(1 + \sigma\eta^2)/V\chi_\sigma \tag{31c}$$

$$\beta_A = -\sigma\eta(1 + \sigma\eta^2)/V\chi_\sigma \tag{31d}$$

$$\beta_B = -\eta(1 + \sigma\eta^2)/V\chi_\sigma \tag{31e}$$

where

$$\zeta = (2z - \varepsilon_A - \varepsilon_B)/2V \tag{32a}$$

$$\varphi = (\varepsilon_A - \varepsilon_B)/2V \tag{32b}$$

and

$$\chi_\sigma = (1 + \sigma\eta^2)(\zeta^2 - \varphi^2) - 2. \tag{33}$$

Unlike the monatomic MNA, where x^{-1} is a reduced energy parameter given by equation (10), we now have x given by equation (31*a*). For fixed η, the mapping from x to the energy parameter ζ has two branches

$$\zeta = \frac{x^{-1}\eta(1+\sigma)}{2} \pm \left[\left(\varphi + \frac{x^{-1}\eta(1-\sigma)}{2}\right)^2 + x^{-2}\eta^2\sigma + x^{-1}(1+\sigma\eta^2)^{-1}(2x+\sigma+3\eta^2)\right]^{1/2} \tag{34}$$

when $x \neq 0$. When $x = 0$ and $\sigma = 1$ (case (a)) we have

$$\zeta = -(1+3\eta^2)/[2\eta(1+\eta^2)]. \tag{35}$$

The line $x = 0$ is an invariant line in the (x, η) plane. It contains the attractive fixed point $x = \eta = 0$ and corresponds to the special case of a non-interacting system.

In the (x, η) plane the band edges are given, from equations (14), by the expression $x = (\pm 1 - \eta^2)/2$ and substituting in equation (34) we have two bands with edges $(\zeta_+^{(1)}, \zeta_+^{(2)})$ and $(\zeta_-^{(1)}, \zeta_-^{(2)})$ given by

$$\zeta_\pm^{(1)} = \frac{\eta(1+\sigma)}{1-\eta^2} \pm \left[\left(\varphi + \frac{\eta(1-\sigma)}{1-\eta^2}\right)^2 + \frac{2(1+\sigma)}{(1-\eta^2)^2}\right]^{1/2} \tag{36a}$$

$$\zeta_\pm^{(2)} = -\frac{\eta(1+\sigma)}{1+\eta^2} \pm \left(\varphi^2 + \frac{2(1-\sigma)(1-\varphi\eta)}{1+\eta^2}\right)^{1/2}. \tag{36b}$$

These band edges were obtained by Davison (1972), except that he omitted the modulus signs which occur in equations (36*a*) and (36*b*) when $\sigma = -1$ and $\sigma = 1$ respectively. This led him to believe that in case (b) ($\sigma = -1$) the band edges $\zeta_\pm^{(1)}$ crossed at $\zeta = 0$, leading to an overlap of bands. In fact the bands touch at the point $\zeta = 0$, $\eta = [1 - (1+\varphi^2)^{1/2}]/\varphi$ where the band edges have a discontinuity of slope.

For case (a) the width of the band becomes zero when $\eta = \mp \eta^*(\varphi)$, where η^* is the one real root of

$$2\eta^3|\varphi| + \eta^2 + 2\eta|\varphi| - 1 = 0 \tag{37a}$$

in the range $(-1, 1)$. Substituting back into equations (36), with $\sigma = 1$, we find that the points of zero band width occur at $\zeta = \pm\zeta^*(\varphi)$, where

$$\zeta^* = (1+3\eta^{*2})/[2\eta^*(1+\eta^{*2})]. \tag{37b}$$

For case (b) the cubic equation

$$2\varphi\eta^3 - 3\eta^2 - 2\varphi\eta + 1 = 0 \tag{38a}$$

has two real roots $\eta_1(\varphi)$ and $\eta_2(\varphi)$ in the range $(-1, 1)$ and the band width of each band is zero at both η_1 and η_2 where

$$\zeta = \zeta_i(\varphi) = \pm[\varphi^2 - 2(1-\eta_i^2)^{-1}]^{1/2} \qquad i = 1, 2. \tag{38b}$$

The reason for which it is possible to obtain points of zero band width using a mapping from the (x, η) plane, where the band is always of non-zero width, is clear if we substitute from equations (37) and (38) into equation (31*a*), when it is seen that both the numerator and denominator are zero.

In general it is not possible to obtain the diagonal GF for the system by transforming equation (18) in the same way as we have transformed (14) to obtain the band edges.

The reason for this is that, in equations (31), the initial values of β_A and β_B are non-zero leading to a non-equivalence between this model and the homogeneous monatomic chain. In the special case $\eta = 0$, however, this non-equivalence is removed and the scaling equations reduce to the NN case given by equations (12) with $\rho = 0$, $\alpha_0 = \alpha_0^{(A)}$, $\alpha_0^{(B)}$, $\beta = \beta_A, \beta_B$. If in equations (18) we substitute $\rho = 0, x$ given by equation (31*a*) and $\alpha_0^{(A)}$ and $\alpha_0^{(B)}$ given by equations (31*b*) and (31*c*), successively for α_0, we obtain for both cases (a) and (b)

$$G_{AA}(0,0) = \frac{1}{V}\left(\frac{\zeta + \varphi}{(\zeta - \varphi)(\zeta^2 - \varphi^2 - 4)}\right)^{1/2} \tag{39a}$$

$$G_{BB}(0,0) = \frac{1}{V}\left(\frac{\zeta - \varphi}{(\zeta + \varphi)(\zeta^2 - \varphi^2 - 4)}\right)^{1/2}. \tag{39b}$$

The partial DOS $D_C(E)$ at a C site, for C = A, B, is given by

$$D_C(E) = -\lim_{\theta \to 0+} \pi^{-1} \operatorname{Im}[G_{CC}(0,0;z)] \tag{40}$$

where $z = E + i\theta$. When $\eta = 0$ the band-edge equations (36) take the simple form

$$\zeta_{\pm}^{(1)} = \pm[\varphi^2 + 2(1+\sigma)]^{1/2} \tag{41a}$$

$$\zeta_{\pm}^{(2)} = \pm[\varphi^2 + 2(1-\sigma)]^{1/2}. \tag{41b}$$

For case (a) ($\sigma = 1$) both partial DOS have square-root singularities at the band edges $\zeta_{\pm}^{(1)}$ and at the band edges $\zeta_{\pm}^{(2)}$ there is one zero and one square-root singularity for each partial DOS. For case (b) ($\sigma = -1$) the roles of $\zeta_{\pm}^{(1)}$ and $\zeta_{\pm}^{(2)}$ are reversed. Curves for partial DOS, derived from these formulae, are given by Parent *et al* (1980). For η non-zero the scaling procedure is used to obtain partial DOS. We find that the band-edge properties are unchanged by the introduction of η.

Band-edge curves for the s-orbital model (case (a)) for $\varphi = 1$ are given by Davison (1972). For this case equations (37) give the numerical values $\eta^*(1) = 0.376$, $\zeta^*(1) = 1.659$. In figure 2 we present curves for the partial DOS of the s-orbital model plotted against $\zeta = (2E - \varepsilon_A - \varepsilon_B)/2V$ for $\eta = 0.6$, $\varphi = 1$. The band edges are $(\zeta_-^{(2)}, \zeta_-^{(1)}) = (-1.883, -1.402)$, $(\zeta_+^{(2)}, \zeta_+^{(1)}) = (0.118, 5.158)$. Each partial DOS has a square-root singularity at the upper band edge. As η is decreased through η^* the band edges of the lower band are reversed and at $\eta = 0$ we have the results of Parent *et al* (1980) where the square-root singularities of both partial DOS occur at the pair of outer band edges. In figure 3 we present another example of the s-orbital model with $\eta = 0.6$, $\varphi = 1$, $\bar{V}_{AA} = V$, $\bar{V}_{BB} = 0.5V$. Here the initial value of y, given by equation (23*b*), is no longer zero and the analytic derivation of the band edges, given above, no longer applies. The situation is somewhat similar to that of the s–p hybrid crystal discussed in § 5. The parameter y for $\eta = 0$ becomes a next-NN interaction, which generates internal band singularities. When $\eta \neq 0$ these effects persist.

In figure 4 we present the partial DOS for the s–p-orbital model (case (b)) when $\eta = 0.6$, $\varphi = 1$. In this case the bands touch at $\eta = -0.414$ and, from equations (38), $\eta_1(1) = -0.745$, $\eta_2(1) = 0.4$ with $\zeta_1(1) = \pm 2.344$, $\zeta_2(1) = \pm 1.839$. Each partial DOS has a square-root singularity at the inner band edge.

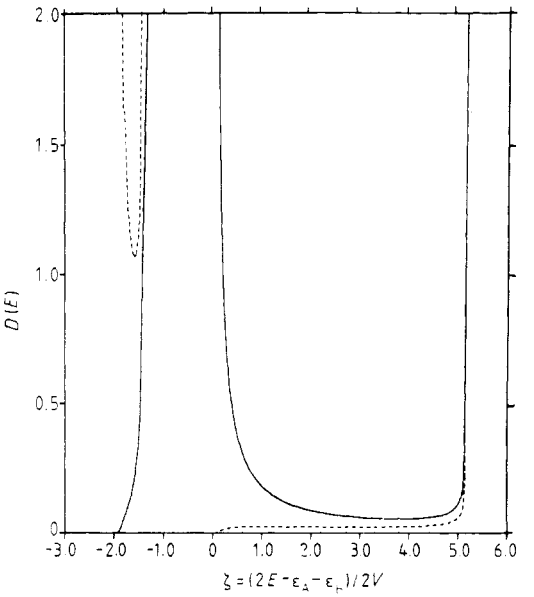

Figure 2. Partial densities of states for the s-orbital model of a diatomic crystal, plotted against $\zeta = (2E - \varepsilon_A - \varepsilon_B)/2V$. The parameter values are $\eta = 0.6$ ($\rho = 0.36$), $V_{AB} = V_{BA} = V = 1.0$, $\bar{V}_{AA} = \bar{V}_{BB} = 1.0$, $\varphi = 1.0$. The partial densities of states for A and B atoms are represented by full and broken curves respectively.

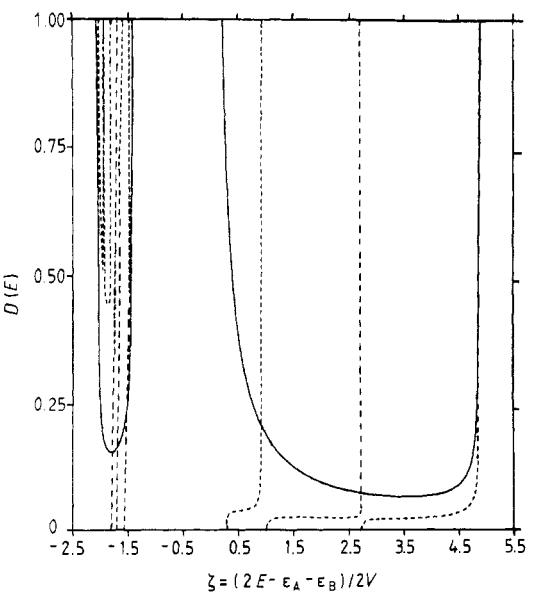

Figure 3. The same as in figure 2 except that $\bar{V}_{AA} = 1.0$, $\bar{V}_{BB} = 0.5$.

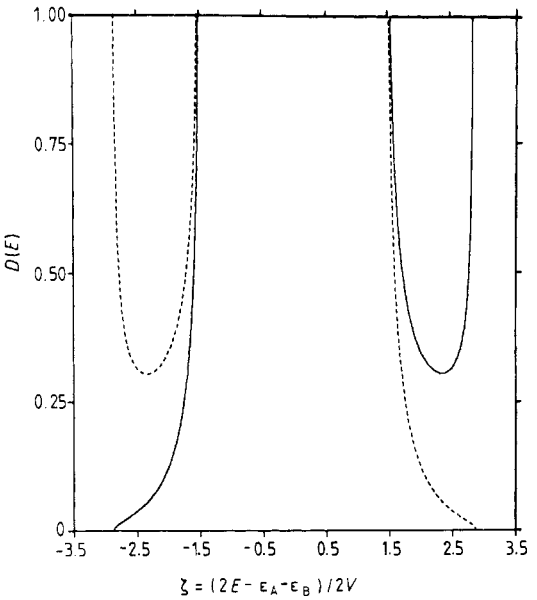

Figure 4. Partial densities of states for the s–p-orbital model of a diatomic crystal, plotted against $\zeta = (2E - \varepsilon_A - \varepsilon_B)/2V$. The parameter values are $\eta = 0.6$ ($\rho = 0.36$), $V_{AB} = -1.0$, $V_{BA} = V = 1.0$, $\bar{V}_{AA} = 1.0$, $\bar{V}_{BB} = -1.0$, $\varphi = 1.0$. The convention for representing curves is the same as in figures 2 and 3.

5. An s–p hybrid model

For the ionic crystal, described in § 4, the s and p orbitals are located at alternate sites. In an s–p hybrid crystal like silicon or germanium both orbitals are located on the same site. In this case, therefore, we construe the A and B sites of figure 1 as s and p orbitals respectively and a pair as representing a single atom. The model of § 3 is applicable to that situation in all its generality. For ease of discussion, however, we shall concentrate on the special case $\varepsilon_A = \varepsilon_B = \varepsilon_0$, $V_{AA} = V_{BB} = V$ which was investigated by Davison and Foo (1976). When $\rho = 0$, it follows from equation (22*a*) that x and y become the NN and next-NN interactions ($x = x_1$, $y = x_2$) and the scaling equations reduce to

$$x' = (x^2 + 2y)/(1 - 2x^2 + 2y^2) \tag{42a}$$

$$y' = -y^2/(1 - 2x^2 + 2y^2) \tag{42b}$$

$$\alpha_0^{(C)\prime} = (\alpha_0^{(C)} + 2x\beta_C)/(1 - 2x^2 + 2y^2) \qquad C = A, B \tag{42c}$$

$$\beta_C' = (\beta_C x - \alpha_0^{(C)} y)/(1 - 2x^2 + 2y^2) \qquad C = A, B. \tag{42d}$$

The next-NN problem has been considered by Southern *et al* (1983b) and the DOS has been calculated by Bahurmuz and Loly (1981). In the (x, y) plane the line

$$2y + 2x = 1 \tag{43a}$$

and the curve

$$(4y + 1)^2 = 1 - 2x^2 \tag{43b}$$

are invariant under the transformation (42) and the line

$$2y - 2x = 1 \tag{43c}$$

maps into equation (43*a*) in one iteration. The band of extended states is given by $x_L^{-1} \leqslant x^{-1} \leqslant x_U^{-1}$, where

$$x_L^{-1} = \begin{cases} 2(y/x) - 2 & (y/x) \leqslant \frac{1}{4} \\ -[1 + 8(y/x)^2]/(4y/x) & \frac{1}{4} \leqslant (y/x) \end{cases} \tag{44a}$$

$$x_U^{-1} = \begin{cases} -[1 + 8(y/x)^2]/(4y/x) & (y/x) \leqslant -\frac{1}{4} \\ 2(y/x) + 2 & -\frac{1}{4} \leqslant (y/x). \end{cases} \tag{44b}$$

The band edge $x = x_U$ contains the fixed point $x = \frac{1}{2}$, $y = 0$, which is the ordinary band-edge fixed point encountered in our discussion of the monatomic system, and the fixed point $x = \frac{2}{3}$, $y = -\frac{1}{6}$ which is a special point located at the meeting of the two different analytic forms for x_U in equation (44*b*). The corresponding points $x = -\frac{1}{2}$, $y = 0$ and $x = -\frac{2}{3}$, $y = -\frac{1}{6}$, which lie on x_L, are mapped into the fixed points in one iteration. We now define the variables

$$\zeta = (z - \varepsilon_0)/V \tag{45a}$$

$$\nu = V_{BA}/V \tag{45b}$$

$$\xi = V_{AB}/V \tag{45c}$$

and obtain the band edges of the s–p hybrid (for $\rho = 0$) using the mapping given by equations (23*a*) and (23*b*). These equations can be re-expressed in the form

$$x = (2\zeta + \xi\nu)/(2 + \zeta^2 - \xi^2 - \nu^2) \tag{46a}$$

$$y = -1/(2 + \zeta^2 - \xi^2 - \nu^2). \tag{46b}$$

For fixed ξ, the mapping from the (x, y) plane to the (ζ, ν) plane is two-valued. We restrict ourselves to the case of non-negative ξ and ν. On physical grounds, it is also reasonable to restrict ξ further to the range $\xi > 1$. We find that the topology of the band edges differs substantially according as $\xi > 2$ or $2 > \xi > 1$. Figure 5(*a*) represents a typical case ($\xi = 3.0$) for $\xi > 2$. We have two distinct bands which touch at the point A given by $(\nu, \zeta) = (\xi, -2)$. On the upper edge of the lower band the point C is given by $(\nu, \zeta) = (2, -\xi)$. On the lower edge of the lower band the points B′ and B are given by

$$\text{B}': (\nu, \zeta) = (2\xi, -\xi^2 - 2\xi - 4)/(2 + \xi) \tag{47a}$$

$$\text{B}: (\nu, \zeta) = (2\xi, -\xi^2 + 2\xi - 4)/(\xi - 2). \tag{47b}$$

Between these points the analytic form of the band edge is

$$y = -\tfrac{1}{4}\xi\nu - \xi/\nu - \nu/\xi. \tag{48}$$

The point B is an image of the fixed point $x = \frac{2}{3}$, $y = \frac{1}{6}$ and B′ is an image of $x = -\frac{2}{3}$, $y = -\frac{1}{6}$. The broken lines within the band correspond to internal singularities of the partial DOS.

In figure 6(*a*) the DOS corresponding to the lower band of figure 5(*a*), when $\xi = 3.0$, $\nu = 2.1$, is shown. The partial DOS for the s and p orbitals coincide whenever, as in this case, $V_{AA} = V_{BB}$. The band edges in figure 5(*a*) where obtained by Davison and Foo

(1976), except that they failed to obtain the portion of the band enclosed between the broken lines and the curve B′B. They, therefore, deduced that the band contracted to zero width at C.

The band structure for a typical case with $1 < \xi < 2$ ($\xi = 1.5$) is given in figure 5(*b*). Here there is only one band for $\nu < 2$ and the point A, where the band splits, is given by $(\nu, \zeta) = (2, -\xi)$. The point B′ is again given by equation (47*a*) and B by

$$\text{B: } (\nu, \zeta) = (2\xi, 2\xi - \xi^2 - 4)/(2 - \xi). \tag{49}$$

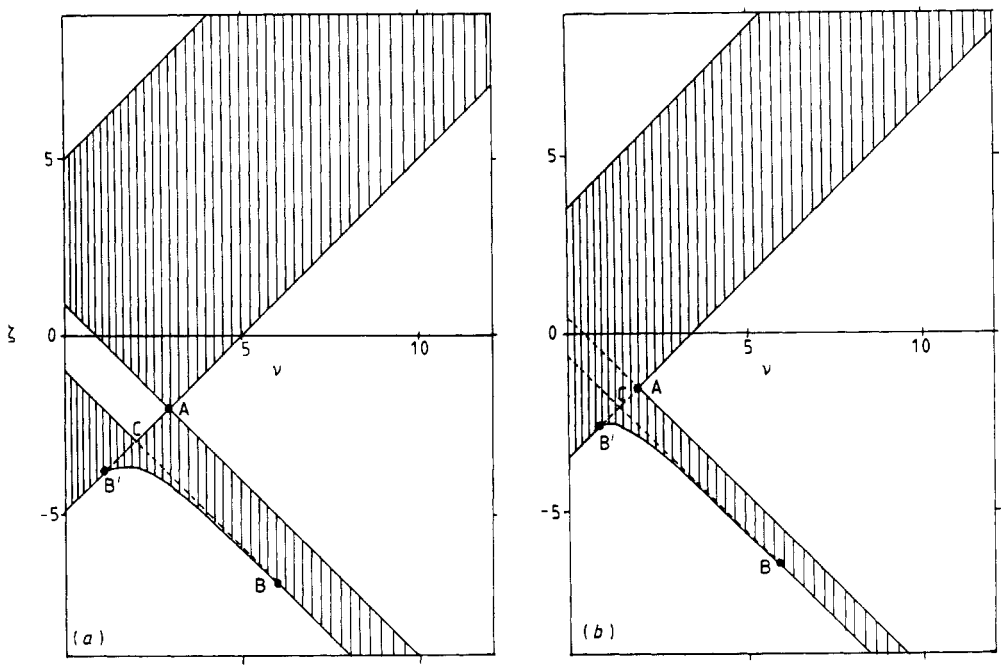

Figure 5. Band edges for the s–p hybrid crystal with (*a*) $\xi = 3.0$, (*b*) $\xi = 1.5$. The broken lines represent internal singularities in the bands.

The band edge between B′ and B is given by equation (48). In this case we have up to three internal singularities in the band for fixed ν. The point C, where the internal singularities cross, is $(\nu, \zeta) = (\xi, -2)$. B and B′ are both images of the point $x = -\frac{2}{3}$, $y = -\frac{1}{6}$. The partial DOS for this case, with $\xi = 1.5$, $\nu = 1.3$ is shown in figure 6(*b*).

Although the presence of a non-zero value of ρ affects the location of the band edges the same qualitative behaviour is observed. We do, however, obtain a more complicated form of DOS when $V_{AA} \neq V_{BB}$. The partial DOS for the s and p orbitals no longer coincide and when $V_{AA} > V_{BB}$, more internal singularities occur in the partial DOS for the p orbital. An example of this is given in figure 7, with $\rho = 0.5$, $\nu = 2.0$, $\xi = 1.5$, $V_{AA} = V$, $V_{BB} = 0.5\,V$.

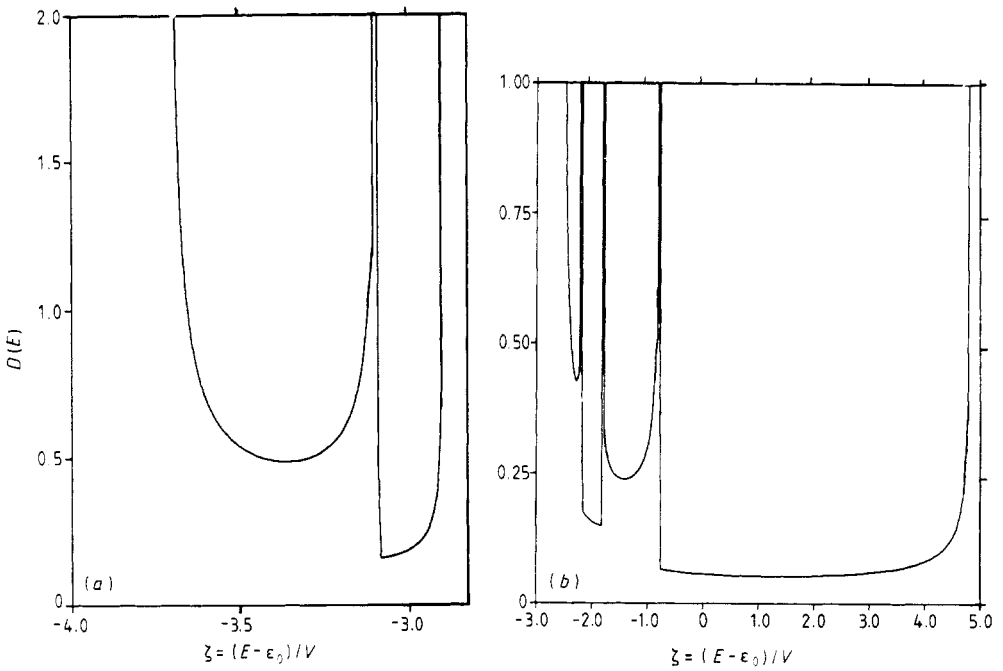

Figure 6. Density of states for the s–p hybrid model, plotted against $\zeta = (E - \varepsilon_0)/V$. The parameter values are $\rho = \varphi = 0$ and in (*a*) $V_{AB} = 3.0$, $V_{BA} = 2.1$ (where only the band of lower energy is shown) and in (*b*) $V_{AB} = 1.5$, $V_{BA} = 1.3$. In this case the partial densities of states for the s and p orbitals coincide.

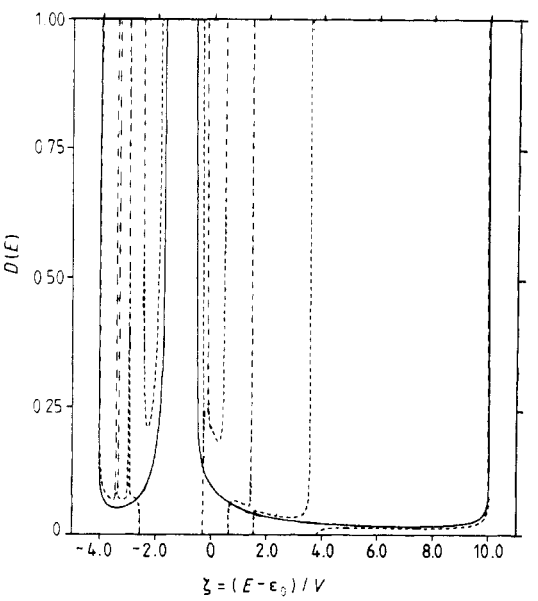

Figure 7. Partial densities of states for the s–p hybrid crystal, plotted against $\zeta = (E - \varepsilon_0)/V$, with parameter values $\varphi = 0$, $\rho = 0.5$, $V_{AA} = V = 1.0$, $V_{BB} = 0.5$, $V_{AB} = 1.5$, $V_{BA} = 2.0$. The full and broken curves correspond respectively to the partial densities of states for the s and p orbitals.

6. Conclusions

We have considered a generalised diatomic tight-binding system in the MNA, to which we apply a transformation, which decouples it into two monatomic systems with more complicated interactions. In some special cases this allows us to obtain analytic results directly from those for the simple monatomic MNA. In general it is possible, at this stage, to use traditional Fourier transform methods to complete the calculations (Bahurmuz and Loly 1981, Shen 1985). This procedure is relatively tedious for anything more than the NN problem and we have used an alternative rescaling method, which allows us to obtain partial DOS in a simple way. Our method also has the advantage of affording us some physical insights into the problem. We find, for example, that under iteration the many-neighbour parameter ρ scales to zero. This shows that the physical behaviour of the systems considered is primarily determined by the finite-range problems. Our method is applied to both diatomic crystals and an s–p hybrid system.

Acknowledgments

Two of the authors (DAL and BWS) acknowledge the support of Nato Research Grant No 033.80. This work was also supported by the Natural Sciences and Engineering Research Council of Canada. In particular one of us (SGD) wishes to thank NSERC and the Royal Society of London for a grant, under the auspices of the Anglo-Canadian Scientific Exchange Scheme, which enabled him to enjoy the hospitality of the Department of Mathematics at Chelsea College, London. The authors have also benefited from discussions with P D Loly.

References

Bahurmuz A A and Loly P D 1981 *J. Math. Phys.* **22** 564–8
Davison S G 1972 *Int. J. Quantum Chem.* **6** 387–93
Davison S G and Foo E-N 1976 *Int. J. Quantum Chem.* **10** 867–72
Davison S G, Lavis D A and Sulston K W 1986 *J. Phys. Chem.* **90** 652–5
Davison S G and Taylor N F 1969 *Chem. Phys. Lett.* **3** 424–6
Economou E N 1983 *Green's Functions in Quantum Physics, Springer Series in Solid State Sciences* vol 7, 2nd edn (Berlin: Springer)
Langlois J-M, Tremblay A-M S and Southern B W 1983 *Phys. Rev.* B **28** 218–31
Lavis D A, Southern B W and Davison S G 1985 *J. Phys. C: Solid State Phys.* **18** 1387–99
Parent L G, Davison S G and Ueba H 1980 *J. Electroanal. Chem.* **113** 51–62
Shen Y 1985 *Physica* B **133** 43–54
Southern B W, Kumar A A and Ashraff J A 1983a *Phys. Rev.* B **28** 1785–91
Southern B W, Kumar A A, Loly P D and Tremblay A-M S 1983b *Phys. Rev.* B **27** 1405–8
Tremblay A-M S and Southern B W 1983 *J. Physique. Lett.* **44** L845–52